# Shaping ability of ProTaper nickel-titanium files in simulated resin root canals

**F. L. G. Calberson, C. A. J. G. Deroose, G. M. G. Hommez & R. J. G. De Moor**

Department of Operative Dentistry and Endodontology, Dental School, Ghent University, Ghent University Hospital, Gent, Belgium

## Abstract

**Calberson FLG, Deroose CAJG, Hommez GMG, De Moor RJG.** Shaping ability of ProTaper nickel-titanium files in simulated resin root canals. *International Endodontic Journal*, **37**, 613–623, 2004.

**Aim** To determine the shaping ability of ProTaper instruments in simulated root canals.

**Methodology** Forty canals with four different shapes in terms of angle (20° and 40°) and position of curvature (straight section before curve: 8 and 12 mm) were enlarged according to the recommendations of the manufacturer with the finishing files F1, F2 and F3 to full working length. Preoperative and postoperative pictures, recorded using a digital camera, were superimposed and aberrations recorded. Measurements were carried out at five different points: at the canal orifice (O); half-way to the orifice in the straight section (HO); beginning of the curve (BC); apex of the curve (AC); end-point (EP).

**Results** Ten instruments deformed (nine F3 and one S1, all in canals with straight section of 8 mm), one instrument fractured. There were significant differences between the various canal shapes for the amount of resin removed from the inner curve at all points (O: $P < 0.05$; HO: $P = 0.001$; BC, AC and EP: $P < 0.001$); and for the resin removed on the outer curve at points HO, AC and EP ($P < 0.001$). Mean transportation was towards the inner aspect of the curve in all canal types at points BC, towards the outer aspect at the end-point of preparation (EP) in all canals with 12 mm straight section. In 8 mm straight section canals, four danger zones were found; in 12 mm straight section canals three zips were present. The canal aberrations were produced following the use of the F2 and F3 instruments. There were no aberrations following the use of the F1 instrument.

**Conclusions** Under the conditions of this study, ProTaper instruments performed acceptable tapered preparations in all canal types. When using F2 and F3 in curved canals, care should be taken to avoid excessive removal at the inner curve, leading to danger zones. In addition, care should also be taken to avoid deformation of the F3 instrument.

**Keywords:** canal shape, nickel-titanium, ProTaper, root canal preparation, rotary instruments, simulated canals.

*Received 31 December 2003; accepted 1 June 2004*

## Introduction

Root canal preparation has two objectives: thorough debridement of the root canal system and the specific shaping of the root canal preparation to receive a filling (Ingle *et al.* 2002). The ideal preparation of the root canal is a funnel shaped form with the smallest diameter at the apex and the widest diameter at the orifice (Schilder 1974). This can be achieved either by classical hand- or by mechanical preparation. Hand preparation techniques can be time consuming, and especially in narrow and curved canals, aberrations, such as ledging, zipping, danger zones and transportation can occur because larger instruments tend to straighten the canal (Esposito & Cunningham 1995, Glosson *et al.* 1995).

Correspondence: Prof. Roeland De Moor, Department of Operative Dentistry and Endodontology, Dental School, Ghent University Hospital, Ghent University, De Pintelaan 185 (P8), B-9000 Gent, Belgium (Tel.: + 32 9 240 41 61; fax: + 32 9 240 38 51; e-mail: roeland.demoor@ugent.be).

In narrow and curved canals, more flexible files made of nickel-titanium have been effective in minimizing complications during preparation (Wu & Wesselink 1995, Zmener & Banegas 1996, Thompson & Dummer 1997). Niti-alloy in this respect, has several advantages over stainless steel such as its greater flexibility due to superelasticity, the shape memory effect and a better resistance to torsional fracture (Walia *et al.* 1988). In the last decade, engine-driven nickel-titanium files were developed. According to Glosson *et al.* (1995) these instruments produce a better centred and rounder canal preparation in comparison with hand operated stainless steel and nickel-titanium K-type files. Rotary nickel-titanium instruments can prepare narrow and severely curved canals in a tapered form with fewer aberrations and more rapidly (Thompson & Dummer 1997). Recently, ProTaper instruments (Dentsply Maillefer, Ballaigues, Switzerland) have been introduced but few reports are available on their effectiveness.

ProTaper instruments consist of one auxiliary shaping file (SX), two shaping files (S1 and S2), and three finishing files (F1–3). The S1 and S2 are designed to prepare mainly the coronal two-thirds of the canal; they also enlarge progressively the apical one-third in small canals. The auxiliary SX file can be used to enlarge the coronal aspect of the root canal and relocate the canal orifice away from furcal danger zones. The SX file should be used in a brushing motion to remove overlying dentine to achieve straight-line radicular access. The shaping of the apical one-third of the canal can be accomplished with the finishing files F1, F2 and F3, whose tip diameters correspond, respectively, with ISO sizes 20, 25 and 30. The ProTaper instruments have a multi-tapered shaft design, and the convex triangular cross-section, without radial lands, give these instruments a cutting rather than a planing action (Ruddle 2001).

The aim of the present study was to investigate the shaping ability of the ProTaper files in curved simulated root canals, to measure the amount of material removed at the different levels in the root canal and to record the aberrations that were created.

## Materials and methods

### Construction of simulated canals

A total of 40 simulated root canals were made in clear resin blocks (Dummer *et al.* 1991). Annealed silver points size 20 were used as root canal templates. Four different canal types were formed by precurving silver points using canal formers. The bent silver points were then checked under magnification (8×) for their alignment to the canal former, and inappropriate points were discarded. Clear spectrophotometer cuvettes were used as moulds to retain the self-polymerizing resin (Stycast 1266; Emerson & Cuming, Westerlo, Belgium) that was poured around the preformed silver points.

In all, 40 simulated canals were constructed, 10 of each with a different shape in terms of angle (either 20° and 40°) and position of curvature (straight section prior to the curve 8 or 12 mm). These four canal types are pictured in Fig. 1. The angle and radius of the curvature were determined according to Pruett *et al.* (1997); the radius was 6 mm.

### Preparation of simulated canals

All canals were prepared with ProTaper instruments (Dentsply Maillefer) using a low torque control motor (ATR Tecnika Torque Control Motor with 16 : 1 reduction Contra Angle; ATR, Pistoia, Italy). Ten canals of each shape were prepared by one and the same operator to a working length of 16 mm using the standard settings incorporated in the ATR software [300 rpm; SX and S1 with torque value setting ($T$) = 99; S2 with $T = 20$; F1 with $T = 28$; F2 with $T = 40$; F3 with $T = 56$]. A new set of instruments was used per canal. The preparation followed the instructions of the manufacturer.

Each rotating instrument was gently moved downwards until light resistance was felt. When necessary, recapitulations with the same file were performed until the appropriate length was achieved. Before reinsertion, the file flutes were wiped off on a gauze to remove resin particles, and the instruments were checked for signs of distortion. A deformed instrument was replaced by a new one. In case of separation or deformation, instrument type and canal type were recorded. On reaching the appropriate preparation length, the instrument was immediately withdrawn. Irrigation with tap water was performed after each file. A size 15 Flexofile (Dentsply Maillefer) was used as patency file. The preparation sequence and depth of preparation were as follows (sequence for long root canals):

1. Shaping file No. 1 (S1) to a depth of 10 mm
2. Auxiliary Shaping file (SX) to a depth of 8 mm
3. Shaping file No. 1 (S1) to full working length (16 mm)
4. Shaping file No. 2 (S2) to full working length (16 mm)

 

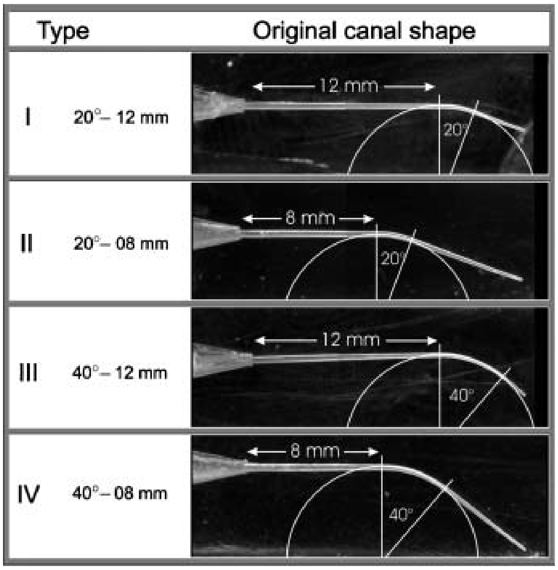


**Figure 1** The four different canal types.

**5–7** Finishing files No. 1 (F1), 2 (F2) and 3 (F3) to full working length (16 mm)

To facilitate handling during preparation, each resin block was placed in a copper holder, masking the entire canal (Calberson *et al.* 2002). Masking the resin blocks ensured that the process was carried out with purely tactile sensation.

### Assessment of canal preparation

The results of the canal preparations were assessed using a digital camera (Fujifilm digital camera Finepix S1 Pro; Fuji Photo Film Co., Tokyo, Japan) with macro lens [120 mm Medical Nikor (1/1) with $f = 4$], connected to a Pentium PC. In order to take standardized and reproducible pictures, a table, on which the camera was placed in a fixed position, was constructed, as well as an adjustable tablet with holder for the resin blocks (Fig. 2). Pre- and postoperative high-resolution pictures of the canals ($3040 \times 2040$ pix) were taken. Due to the experimental magnification of the macro lens (1.5×) the canals were reduced in two segments. These two pictures were accurately aligned with image editing software (Photoshop 6; Adobe Systems Inc., San Jose, CA, USA) and digitally stored.

Prior to the preparation of the resin blocks, the preoperative digital images of the canals were compared with a canal shape template that was constructed with graphical designing software (CorelDraw Version 9.0; Corel Corporation, Ottawa, Ont., Canada). The dimensions of the simulated canal were compared with the predefined dimensions of the template. Only resin blocks with a preoperative canal shape accurately corresponding to the template were used (a maximum error of two pixels on one side of the outline of the canal template was allowed).

Pre- and postoperative pictures were taken and superimposed. Prior to superimposition, using image

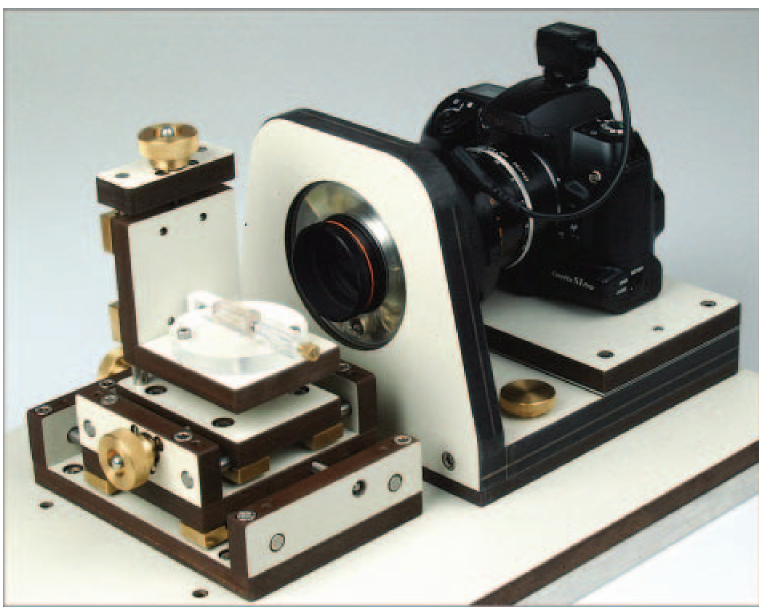

**Figure 2** Imaging system with digital camera and macro lens in fixed position.

editing software (Photoshop 6), the canal shape contours of the images were precisely determined and a colour mode adjustment was made in order to facilitate visualization and further analysis (Fig. 3a,b). Two zones along the canal path, one at the funnel-shaped orifice and one at the tip (apical 2 mm), remained unchanged during preparation of the resin blocks, and these two zones served as reference points for the superimposition of the pre- and postoperative images (Fig. 3c).

Measurements were made on superimposed pre- and postoperative digital images using image analysis software (Sigmascan Pro Image Analysis Version 5.0; SPSS Inc., Chicago, IL, USA). With the use of the corresponding templates as previously described, measuring points could be defined along the canal path: five points were determined on each central canal path, for measuring the canal width, using a modification of the method described by Alodeh & Dummer (1989) (Fig. 3c):

Position O: the canal orifice
Position HO: a point halfway from the beginning of the curve to the orifice
Position BC: the beginning of the curve
Position AC: the apex of the curve of the original canal, determined by the intersection of two lines (one along the coronal aspect of the central white line, and the second along the apical portion of the central white line).
Position EP: end-point of preparation.

Along the whole canal path, starting 1.5 mm from the orifice and ending at the tip, additional measuring points were set every 0.5 mm, resulting in a total of 30 extra measurement positions.

At all these levels, the preoperative width, outer curve widths [i.e. amount of resin (in μm) removed on the outer aspect of the curve along the canal] and inner curve widths [i.e. amount of resin (in μm) removed on the inner aspect of the curve along the canal] were assessed perpendicular to the axis of the central canal path. The central canal path or axis of the original canal was determined by dividing the preoperative width into two halves. In order to express the measurements in micrometers, the exact pixel size was determined by means of an object micrometer (Olympus Objectmicrometer OB-M 1/100 mm; Omnilabo,

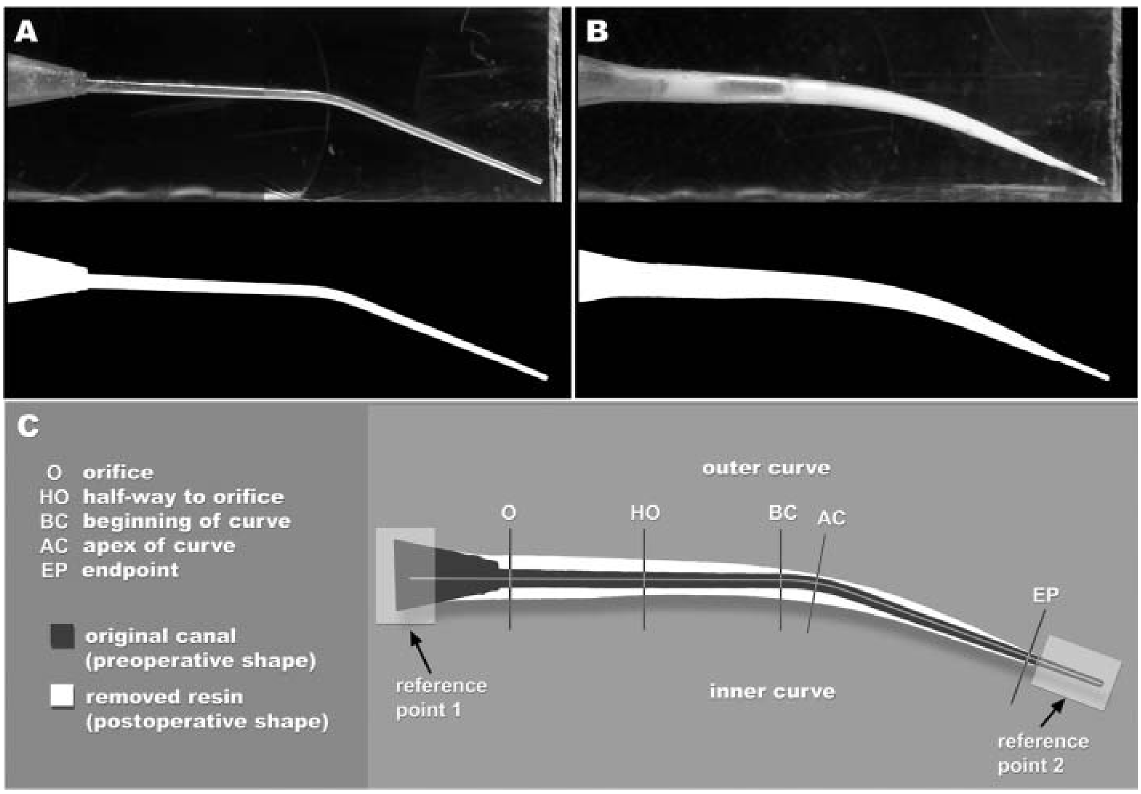


**Figure 3** (a) Preoperative image; (b) post-operative image; (c) superimposed images with the five measuring points along the canal path, and the two reference zones.

 

Aartselaar, Belgium). This is a glass plate with an imbedded scale of precisely 1 mm, with marks every 10 μm. The image calibration was thus performed by grabbing an image of the object micrometer, counting the exact number of pixels in the given distance of 1 mm and calculating the size of one pixel (1 pix = 3.7878 μm). All measurements could then be expressed in μm.

If a canal aberration was present, additional assessments at the corresponding level were made. The canal aberrations to be scored were zips and elbows, ledges, perforations, and danger zones (Alodeh & Dummer 1989) as well as the 'outer widening' (Bryant *et al.* 1999).

At the measuring points O to EP, for each canal, the direction of transportation of the central canal axis was assessed. A transportation was described as a difference between the removal of resin from the inner and outer curve of more than 50 μm. For each canal type, the mean transportation at each of these five measuring points was calculated, and expressed numerically (in μm).

### Recording, storage and analysis of data

All data were stored on PC from the image measuring software directly to a database file. Following error and range checks, the data were analysed using SPSS (SPSS Inc., Chicago, IL, USA), a statistical analysis program. Differences at the five measuring points (O to EP) between the mean total widths, the mean inner curve widths and the mean outer curve widths were statistically analysed using ANOVA, as well as for the differences at the previously described 30 measuring points between the mean total widths, the mean inner curve widths and the mean outer curve widths. A level of $P < 0.05$ was considered significant. Statistical analysis of the number of canals transported towards the inner and outer aspect of the curve was done by means of the Kruskal–Wallis test and a level of $P < 0.05$ was considered significant.

## Results

Because of the presence of one separated instrument (i.e. S1 in a type IV canal), the results are based on the analysis of 39 canals.

### Width measurements and transportation

Tables 1–3 show, respectively, the mean total width, the mean inner curve width and mean outer curve width at points O to EP of the canals by shape. There were statistically significant differences between the various canal types for the amount of resin removed from the inner curve at all points ($P < 0.05$ at point O, $P = 0.001$ at point HO, $P < 0.001$ at points BC, AC and EP), and for the amount of resin removed from the outer curve at the end-point of preparation (EP), the apex of the curve (AC) and halfway to the orifice in the straight section ($P < 0.001$). There were statistically significant differences in the total width of the four canal types at all points ($P < 0.001$) except for the orifice. There were statistically significant differences

**Table 1** Mean total width measurements (mm) of canals by canal shape

| | Type I: 20°, 12 mm (*n* = 10) | Type II: 20°, 8 mm (*n* = 10) | Type III: 40°, 12 mm (*n* = 10) | Type IV: 40°, 8 mm (*n* = 9) | *P*-values |
|---|---|---|---|---|---|
| O Orifice | 1.248 | 1.271 | 1.235 | 1.253 | 0.121 |
| HO Half-way to orifice | 0.968 | 1.057 | 0.959 | 1.115 | 0.000 |
| BC Beginning of curve | 0.687 | 0.864 | 0.673 | 0.893 | 0.000 |
| AC Apex of curve | 0.621 | 0.809 | 0.506 | 0.819 | 0.000 |
| EP 0.3 mm from end-point | 0.423 | 0.365 | 0.432 | 0.368 | 0.001 |

**Table 2** Mean inner width measurements (mm) of canals by canal shape

| | Type I: 20°, 12 mm (*n* = 10) | Type II: 20°, 8 mm (*n* = 10) | Type III: 40°, 12 mm (*n* = 10) | Type IV: 40°, 8 mm (*n* = 9) | *P*-values |
|---|---|---|---|---|---|
| O Orifice | 0.367 | 0.354 | 0.325 | 0.313 | 0.014 |
| HO Half-way to orifice | 0.265 | 0.241 | 0.251 | 0.299 | 0.001 |
| BC Beginning of curve | 0.247 | 0.336 | 0.223 | 0.328 | 0.000 |
| AC Apex of curve | 0.253 | 0.368 | 0.095 | 0.341 | 0.000 |
| EP 0.3 mm from end-point | 0.030 | 0.061 | 0.014 | 0.053 | 0.000 |

**Table 3** Mean outer width measurements (mm) of canals by canal shape

| | Type I: 20°, 12 mm ($n$ = 10) | Type II: 20°, 8 mm ($n$ = 10) | Type III: 40°, 12 mm ($n$ = 10) | Type IV: 40°, 8 mm ($n$ = 9) | $P$-values |
|---|---|---|---|---|---|
| O Orifice | 0.383 | 0.398 | 0.393 | 0.403 | 0.606 |
| HO Half-way to orifice | 0.284 | 0.352 | 0.291 | 0.342 | 0.000 |
| BC Beginning of curve | 0.128 | 0.129 | 0.138 | 0.160 | 0.154 |
| AC Apex of curve | 0.069 | 0.061 | 0.134 | 0.116 | 0.000 |
| EP 0.3 mm from end-point | 0.144 | 0.051 | 0.171 | 0.058 | 0.000 |

between the canal types for the direction of transportation at points AC and EP (Table 4). Mean transportation was towards the inner aspect of the curve in all canal types at points BC (Table 5). At points EP, mean transportation was towards the outer curve in 12 mm canal types, whereas in 8 mm canal types, the mean values indicated no transportation. A representative image for each canal type is pictured in Fig. 4.

The mean values at the 30 measuring points every 0.5 mm along the canal tract are presented in a graph. Figures 5–7 show, respectively, the mean values (in μm) of the inner curve width, outer curve width and total width of the canals by type. Figures 5 and 6 show that canal types with the same onset of the curve have a comparable pattern for the removal of resin. All canal types show a peak in the graph for the removal of resin on the inner curve (Fig. 5). In 12 mm canal types, the peak is reached approximately 1 mm beyond the onset of the curvature, whereas in 8 mm canals the peak values are highest approximately 2 mm beyond the beginning of the curvature. When comparing the peaks in canal types with the same degree of curvature (e.g. type I and II), it can be seen that the distance between the start- and end-points of the peak in 12 mm canals (type I) is less than in 8 mm canals (type II), and that the peak in type I canals runs less symmetrically than in type II canals. This means that in type I canals, resin removal on the inner curve contains only two-thirds of the curvature, whereas in type II there is resin removal from the beginning of the curve until the end of the curvature.

## Instrument evaluation

Instrument failure is characterized either by fracture or by deformation. Table 6 shows the instrument failures in relation to the canal types used in this study. One instrument (S1) fractured in a canal with straight section of 8 mm and 40° curvature. The separation occurred at the middle third of the instrument, with the instrument at full working length, i.e. a separation

**Table 4** Number of canals and their direction of transportation at points A to E by canal type

| | Type I: 20°, 12 mm ($n$ = 10) | | | Type II: 20°, 08 mm ($n$ = 10) | | | Type III: 40°, 12 mm ($n$ = 10) | | | Type IV: 40°, 08 mm ($n$ = 9) | | | |
|---|---|---|---|---|---|---|---|---|---|---|---|---|---|
| | Outer | None | Inner | Outer | None | Inner | Outer | None | Inner | Outer | None | Inner | $P$-values |
| O Orifice | 2 | 8 | 0 | 4 | 6 | 0 | 5 | 4 | 1 | 7 | 2 | 0 | 0.074 |
| HO Halfway straight section | 1 | 8 | 1 | 9 | 1 | 0 | 5 | 5 | 0 | 5 | 4 | 0 | 0.053 |
| BC Beginning of curve | 0 | 0 | 10 | 0 | 0 | 10 | 1 | 1 | 8 | 0 | 1 | 8 | 0.286 |
| AC Apex of curve | 0 | 0 | 10 | 0 | 0 | 10 | 5 | 5 | 0 | 0 | 0 | 9 | 0.000 |
| EP End-point of preparation | 9 | 1 | 0 | 0 | 10 | 0 | 10 | 0 | 0 | 1 | 8 | 0 | 0.000 |

**Table 5** Mean transportation values (in μm) at the five measuring points by canal type (positive value = transportation towards outer curve; negative value = transportation towards inner curve)

| | Type I: 20°, 12 mm ($n$ = 10) | Type II: 20°, 8 mm ($n$ = 10) | Type III: 40°, 12 mm ($n$ = 10) | Type IV: 40°, 8 mm ($n$ = 9) |
|---|---|---|---|---|
| O Orifice | 8 | 22 | 33 | 45 |
| HO Halfway straight section | 10 | 56 | 20 | 25 |
| BC Beginning of curve | −60 | −92 | −43 | −84 |
| AC Apex of curve | −92 | −154 | 19 | −113 |
| EP End-point of preparation | 57 | −5 | 79 | 2 |

 

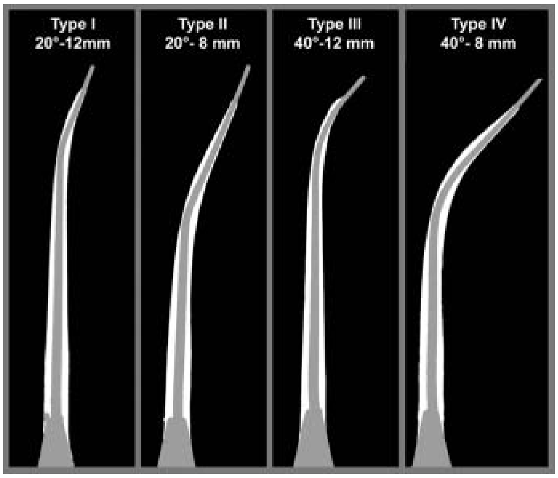


**Figure 4** For each canal type a representative superimposed image is pictured.

located in the beginning of the curve of the canal. A total of 10 instruments deformed (eight F3 and two S1) during preparation; all but one in canal types with straight section of 8 mm (four instruments in a type II canal, five instruments in a type IV canal, one in a type III canal). One S1 deformed at the middle third, another one near the shank. All distorted F3 files deformed in their middle third.

### Canal aberrations

Canal aberrations are listed in Table 6. Aberrations were found in eight simulated canals (20%). Four danger zones were produced (Fig. 8a), all in canal types with 8 mm straight section: three after F2 and four after F3. In canal types with 12 mm straight section, three apical zips were present (two in a 40° canal (Fig. 8b), one in a 20° canal), all after F3. Only one ledge (F2 and F3 in a 40°/8 mm canal) was found. There were no perforations. In canals with a 40° curvature, more aberrations occurred than in 20° canal types.

## Discussion

The purpose of this study was to determine the shaping ability of ProTaper files in curved and simulated root canals. The use of resin blocks was chosen instead of extracted teeth to rule out several parameters that could influence the preparation outcome. The variation in canal anatomy when using extracted teeth is a factor that can aggravate the comparison of the preparation shapes. The hand made simulated canals in resin blocks offer an alternative experimental model with a validity that has been previously described (Lim & Webber 1985). Several advantages, such as the direct visualization of the preparation shape in the clear resin, and the use of canal types with defined shapes in a standardized way, favour the assessment and precision of the measurements. However, because of a difference in hardness between dentine and the experimental resin, care should be taken in extrapolating the results to the clinical situation. The Knoop hardness number of the resin blocks was calculated to be 36; that of dentine

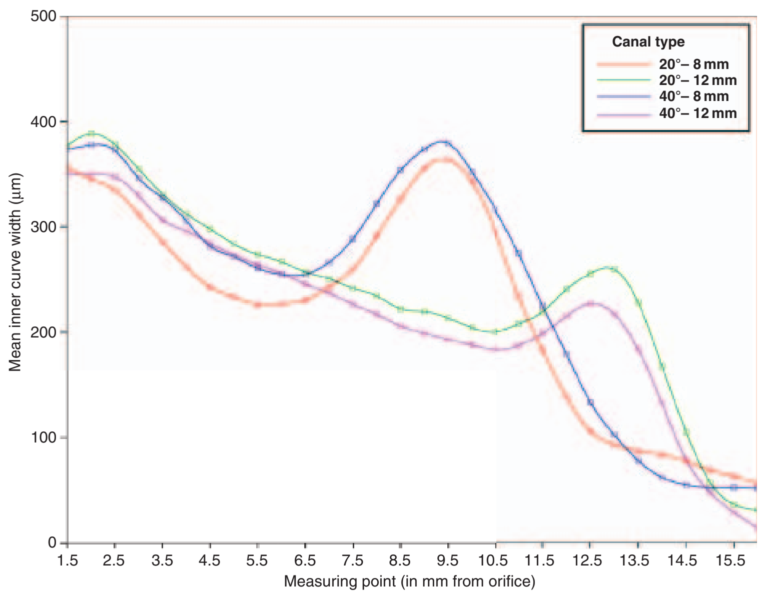


**Figure 5** Mean inner curve widths (μm) at the different measuring points by canal type.

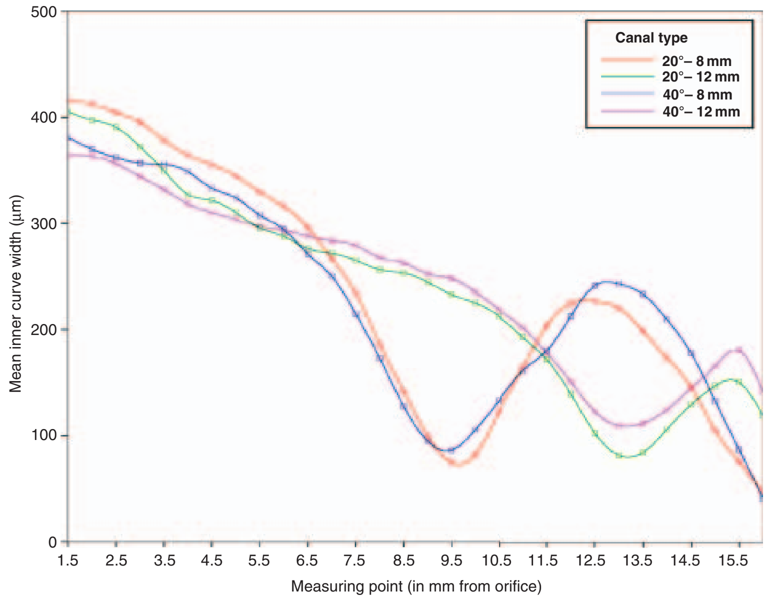


**Figure 6** Mean outer curve widths (µm) at the different measuring points by canal type.

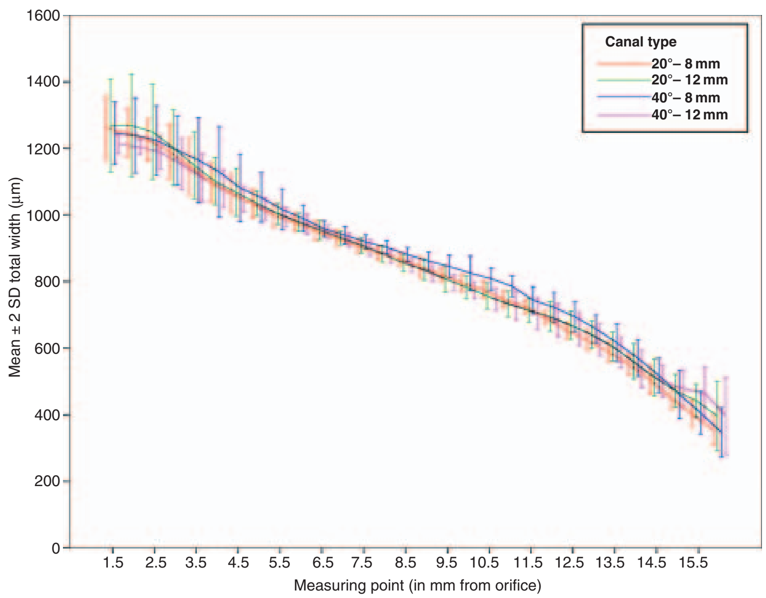


**Figure 7** Mean total curve widths (µm) at the different measuring points by canal type.

has been calculated by Patterson (1963) between 40 and 72.

As hand made resin blocks can differ slightly in shape due to procedural errors during fabrication, a strict routine was adopted when making these blocks. Blocks with simulated canals that did not precisely resemble the predefined shape were excluded. At first, the bent silver points were checked under magnification (8×) for their alignment to the canal former, and inappropriate points were discarded. Furthermore the preoperative images of the canals were compared with the corresponding canal shape template using image analysis software. These four templates, one for each of the four canal types used in this study, represented the theoretical ideal characteristics (in terms of angle of curvature, straight section length and dimension of the size 20 silver point) to which the simulated canals should correspond. Only resin blocks with a preoperative canal shape accurately matching the template, were used. In this way, the construction procedure became more complicated, but all 10 resin blocks in each canal type were found

 

**Table 6** Incidence of instrument failures (by instrument type and location of failure) and canal aberrations by canal type

| | Instrument type and location of failure | Type I: 20°, 12 mm | | | Type II: 20°, 8 mm | | | Type III: 40°, 12 mm | | | Type IV: 40°, 8 mm | | |
|---|---|---|---|---|---|---|---|---|---|---|---|---|---|
| Instrument failure | | | | | | | | | | | | | |
| Fracture | S1 – middle third (1) | 0 | | | 0 | | | 0 | | | 1 | | |
| Deformation | S1 – middle third (1) | 0 | | | 1 | | | 0 | | | 0 | | |
| | S1 – coronal (1) | 0 | | | 0 | | | 0 | | | 1 | | |
| | F3 – midportion (8) | 0 | | | 3 | | | 1 | | | 4 | | |
| | | F1 | F2 | F3 | F1 | F2 | F3 | F1 | F2 | F3 | F1 | F2 | F3 |
| Canal aberrations by instrument type | | | | | | | | | | | | | |
| Apical zip and elbow | | 0 | 0 | 1 | 0 | 0 | 0 | 0 | 0 | 2 | 0 | 0 | 0 |
| Ledge | | 0 | 0 | 0 | 0 | 0 | 0 | 0 | 0 | 0 | 0 | 1 | 1 |
| Danger zone | | 0 | 0 | 0 | 0 | 1 | 1 | 0 | 0 | 0 | 0 | 2 | 3 |

to have simulated root canals equal in size, shape and dimension.

The root canal shaping procedure is complex when relatively nontapered instruments are used to create tapered root canal shapes (Buchanan 2000). With the introduction of more tapered nickel-titanium rotary instruments this difficulty was alleviated and it became possible to produce a better centred and rounder canal preparation when compared with hand operated files (Glosson *et al.* 1995). A modification of the instrument sets containing instruments with different tapers (e.g. 0.02, 0.04, 0.06 taper) is the ProTaper system, which incorporates instruments of progressive multitaper design with sharp cutting blades (Ruddle 2002). The advantage of this progressive taper, whereby only a limited part of the instruments' cutting surface makes contact with the root canal wall, together with the absence of radial lands, is likely to be a reduction of torsional loads on these instruments (Ruddle 2002). A comparative analysis of torsional and bending stresses between ProTaper (with a convex K-file type cross-section) and ProFile (with a concave U-shape cross-section) confirmed the above-mentioned implications in a recent study (Berutti *et al.* 2003). This difference can be of interest in the perspective of instrument distortions and fractures.

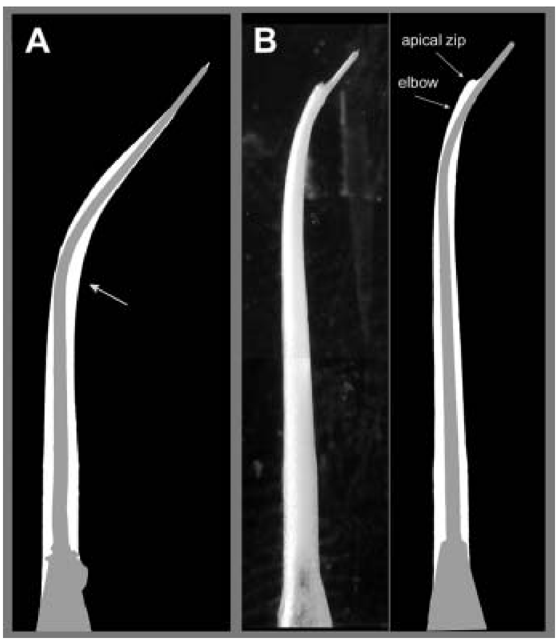


**Figure 8** (a) Composite image of a canal preparation with danger zone (arrow). (b) Composite image of a canal preparation with an apical zip and elbow.

According to the manufacturer, the ProTaper instrumentation should lead to consistent, predictable, and reproducible root canal shaping. In this study, measurements were taken every 0.5 mm to compare the canal shapes between the four different canal types along the whole canal path. Although Figs 5 and 6 show a different shaping pattern between the four canal types for the removal of resin on the inner and outer curve, Fig. 7 shows that the final shape of the four canal types is rather similar. Irrespective of the canal type, the ProTaper preparation can thus be defined as a reproducible and consistent tapered preparation. The difference in shaping patterns on the inner and outer curve in Figs 5 and 6 was more determined by the location of the curvature than by the degree of curvature. Canal types II and IV, with onset of the curvature at 8 mm, showed a similar pattern for the removal of resin on the inner curve, as was the case for 12 mm canal types (I and III). This similarity was also seen in Fig. 6 for the removal on the outer curve. In general the ProTaper files removed more resin on the inner curve at the curvature level. Beyond the curvature, more resin was removed on the outer curve. These findings illustrated the outcome of the measurements at the five different measuring points: at the beginning of the curve (point BC) in all canal types, more resin was removed on the inner curve. This transportation towards the inner curve was bigger in canal types where the curve started at the middle root third (8 mm). In canal types with the curve starting in the apical part (at 12 mm), a typical finding was the transportation at the end-point of preparation to be mainly towards the outer curve, sometimes leading to apical zipping. In these canal types, the majority of the canals showed an unprepared zone apically on the inner curve, a finding that was also seen in a study evaluating the preparation of extracted human maxillary molars (Peters *et al.* 2003a). The latter authors found that the ProTaper preparation left relatively large untreated areas apically at the inner curve and mid-root at the outer curve (data which they expressed by means of percentage of static voxels: depending on the canal type this was 33.2 ± 18.9% for DB canals to 49.0 ± 29.0% for P canals in three-rooted maxillary molars). As these untouched zones were more pronounced in wide canals than in narrower ones, the latter authors suggested that the ProTaper instruments might be better suited for curved and constricted canals than wide, immature ones. Another report (Berutti *et al.* 2003), in which torsional and bending stresses of two theoretical cross-sections [convex (ProTaper) versus concave (ProFile)] were compared, also concluded that the ProTaper files were more indicated to prepare narrow and curved canals, but only during the initial phase of shaping. According to the latter authors, the final shaping in curved canals should better be performed with a U-file design (ProFile) because of its greater elasticity characteristics.

In this study, the majority of the instrument deformations occurred during the final shaping with the Finishing File 3. The same pattern of instrument distortion was seen in another study on simulated canals (Yun & Kim 2003), in which 50% of the F3 files deformed. An explanation was found in the taper of the instruments as result of the multitaper design. The ProTaper finishing files (F1, F2 and F3) have progressively different parabolic tapers. The rate of increase in the diameter of the tip is therefore greater than that of other rotary files (Yun & Kim 2003) and the result is a thicker instrument especially at the apical third of the instrument when compared with other instruments with the same apical size. With a taper of 0.09% the F3 performs like the 0.04/45, 0.04/50, or 0.06/40 instruments at the apical third of the canal. The stiffness of the file and the resistance of the resin block may result in an unwinding of the instrument. In the present study, as in the study of Yun & Kim (2003) no instrument failure was found in the F2 file, which is smaller than an F3 file. The present findings thus suggest that care should be taken when performing the final shaping with F3 files in curved canals or that nickel-titanium files of less taper should be better used for the refining of the apical portion of small curved canals.

Two deformed and one fractured S1 file were noted. The two deformations were recorded without achieving full working length. The fracture of the S1 file occurred after achieving full working length and during retraction of the file. As stated by Peters *et al.* (2003b), not only apically exerted force but also the preoperative canal volume is of importance for torsional load, cyclic fatigue and consequent instrument deformation. These authors, in this respect, emphasized the need for canal enlargement prior to the use of ProTaper instruments at working length. The S1 file in particular gave the widest range in cyclic fatigue and stress profile, and appears therefore to be the instrument the most susceptible to deformation and to be handled with care.

Both physical parameters during shaping (e.g. instrument diameter, torsional load, number of rotations per canal, increment of cyclic fatigue) and canal geometry (e.g. canal angle radius, cross-sectional diameter) determine the amount of stress the instruments have been subjected to (Peters *et al.* 2003a,b). The effect of canal geometry on instrument deformation was confirmed in the present study, as canals type II and IV resulted in the majority of the instrument deformations (90.9%). These canals have the shorter straight section of 8 mm in common when compared with the 12 mm of canals type I and III.

Theoretically, shaping aberrations would be expected to increase as canal curvature increases and as file flexibility decreases (ElDeeb & Boraas 1985). In this study, the majority of the aberrations occurred in 40° curvature canal types, and were more pronounced than in 20° canal types. As a nickel-titanium instrument tends to straighten when rotating in a curved canal, the ProTaper instruments, with their active design, can remove tissue excessively when left in the canal too long. It is therefore of utmost importance to follow the instructions of the manufacturer, and not to leave the instrument prepare the root canal for longer than 1 s when reaching the desired depth. In this way aberrations like danger zones and zips can be prevented. The aberrations found in this study were produced following the use of the F2 and F3 instruments. The preparation from F1 up to F3 instrument tended to straighten canals with an 8 mm straight section. The aberrations, however, were limited in size, and could not always be detected by visual inspection alone. Nevertheless, care should be taken when using the F2 instrument and especially the F3 instrument.

## Conclusion

Under the conditions of this study ProTaper instruments prepared canals in resin blocks to a reproducible and smooth tapered shape. In narrow and curved canals the length of the straight section of the canal determined the direction of transportation more than the angle of the curve. Regardless the canal type used in this study, ProTaper instruments removed more resin on the inner side of the curvature in comparison with the outer side of the curvature. Under the conditions of the present study ProTaper instruments produced aberrations following use of the F2 and F3 instruments. Care should be taken with these instruments to avoid excessive removal at the inner curve, leading to danger zones and straightening of the canal. The aberrations, however, that occurred were minimal in size. When using F3 in curved canals, care should also be taken to avoid instrument deformations.

## References


Alodeh MHA, Dummer PMH (1989) A comparison of the ability of K-files and Hedström files to shape simulated root canals in resin blocks. *International Endodontic Journal* **22**, 226–35.

Berutti E, Chiandussi G, Gaviglio I, Ibba A (2003) Comparative analysis of torsional and bending stresses in two mathematical models of nickel-titanium rotary instruments: ProTaper versus Profile. *Journal of Endodontics* **29**, 15–9.

Bryant ST, Dummer PMH, Pitoni C, Bourba M, Moghal S (1999) Shaping ability of .04 and .06 taper ProFile rotary nickel-titanium instruments in simulated root canals. *International Endodontic Journal* **32**, 155–64.

Buchanan LS (2000) The standardized-taper root canal preparation – part 1. Concepts for variably tapered shaping instruments. *International Endodontic Journal* **33**, 516–29.

Calberson FLG, Deroose CAJG, Hommez GMG, Raes H, DeMoor RJG (2002) Shaping ability of GT™ Rotary Files in simulated resin root canals. *International Endodontic Journal* **35**, 607–14.

Dummer PMH, Alodeh MHA, Al-Omari MAO (1991) A method for the construction of simulated canals in clear resin blocks. *International Endodontic Journal* **24**, 63–6.

ElDeeb ME, Boraas JC (1985) The effect of different files on the preparation shape of severely curved canals. *International Endodontic Journal* **18**, 1–7.

Esposito PT, Cunningham CJ (1995) A comparison of canal preparation with nickel-titanium and stainless steel instruments. *Journal of Endodontics* **21**, 173–6.

Glosson CR, Haller RH, Dove SB, Del Rio CE (1995) A comparison of root canal preparations using Ni-Ti hand, Ni-Ti engine-driven and K-Flex endodontic instruments. *Journal of Endodontics* **21**, 146–51.

Ingle JI, VanHimel T, Harvish CE et al. (2002) Endodontic cavity preparation. In: Ingle JI, Bakeland LF, eds. *Endodontics*, 5th edn. Hamilton–London: BDC Decker Inc., pp. 405–570.

Lim KC, Webber J (1985) The validity of simulated root canals for the investigation of the prepared root canal shape. *International Endodontic Journal* **18**, 240–6.

Patterson SS (1963) In vivo and in vitro studies of the effect of the disodium salt of ethylenediamine tetra-acetate on human dentin and its endodontic implications. *Oral Surgery Oral Medicine Oral Pathology* **16**, 83–103.

Peters OA, Peters CI, Schönenberger K, Barbakow F (2003a) ProTaper rotary root canal preparation: effects of canal anatomy on final shape analysed by micro CT. *International Endodontic Journal* **36**, 86–92.

Peters OA, Peters CI, Schönenberger K, Barbakow F (2003b) ProTaper rotary root canal preparation: assessment of torque and force in relation to canal anatomy. *International Endodontic Journal* **36**, 92–9.

Pruett JP, Clement DJ, Carnes DL (1997) Cyclic fatigue testing of nickel-titanium endodontic instruments. *Journal of Endodontics* **23**, 77–85.

Ruddle C (2001) The ProTaper endodontic system: geometries, features and guidelines for use. *Dentistry Today* **20**, 60–7.

Ruddle C (2002) Cleaning and shaping the root canal system. In: Cohen S, Burns RC, eds . *Pathways of the Pulp*, 8th edn. St Louis, MO: Mosby, pp. 231–92.

Schilder H (1974) Cleaning and shaping the root canal. *Dental Clinics of North America* **18**, 269–96.

Thompson SA, Dummer PMH (1997) Shaping ability of Profile .04 taper series 29 rotary nickel-titanium instruments in simulated root canals. Part 1. *International Endodontic Journal* **30**, 1–7.

Walia H, Brantley WA, Gerstein H (1988) An initial investigation of the bending and torsional properties of Nitinol root canal files. *Journal of Endodontics* **14**, 346–57.

Wu MK, Wesselink PR (1995) Efficacy of three techniques in cleaning the apical portion of curved root canals. *Oral Surgery Oral Medicine Oral Pathology* **79**, 492–6.

Yun H, Kim SK (2003) A comparison of the shaping abilities of 4 nickel-titanium rotary instruments in simulated root canals. *Oral Surgery Oral Medicine Oral Pathology* **95**, 228–33.

Zmener O, Banegas G (1996) Comparison of three instrumentation techniques in the preparation of simulated curved root canals. *International Endodontic Journal* **29**, 315–9.